Res Chem Intermed
https://doi.org/10.1007/s11164-018-3395-z

Diorganotin(IV) complexes of Schiff bases derived from salicylaldehyde and 2-amino-6-substituted benzothiazoles: synthesis, spectral studies, in vitro antimicrobial evaluation and QSAR studies

Aarti Ahlawat[1] · Priyanka Khatkar[1] · Vikramjeet Singh[2] · Sonika Asija[1]

Received: 4 January 2018 / Accepted: 15 March 2018

Abstract In the present work, Schiff base ligands (**1–4**) were prepared by condensation of 2-amino-6-substituted-benzothiazole and salicyaldehyde in a 1:1 molar ratio and were further treated with diorganotindichloride R'_2SnCl_2 leading to a series of organotin(IV) complexes (**5–20**) of type $R'_2SnL^{1-4}Cl$ [R' = Ph, Bu, Et, Me]. The prepared Schiff base ligands and the organotin(IV) complexes were characterized by various spectroscopic techniques (^1H, ^{13}C, ^{119}Sn NMR, FT-IR) and physical techniques. All the synthesized compounds were evaluated for in vitro antibacterial and antifungal activity against two Gram positive bacterial strains *B. cereus*, *S. aureus*, two Gram negative bacterial strains *E. coli*, *P. aeruginosa* and two fungal strains *A. niger* and *A. flavus* by serial dilution method. The spectral data revealed that the complexes were pentacoordinated with bidentate ligands coordinated through oxygen and nitrogen. The results of antimicrobial activity revealed that the synthesized complexes were more toxic towards Gram positive bacterial strains as compared to Gram negative bacterial strains. From the results of QSAR analysis, it was indicated that the antimicrobial activity of the synthesized compounds were controlled by topological parameters (molecular connectivity indices).

Keywords Schiff base ligands · Organotin(IV) complexes · Benzothiazole derivatives · Antimicrobial activity · QSAR studies

Electronic supplementary material The online version of this article (https://doi.org/10.1007/s11164-018-3395-z) contains supplementary material, which is available to authorized users.

✉ Sonika Asija
sc_ic2001@yahoo.co.in

[1] Department of Chemistry, G.J. University of Science and Technology, Hisar, Haryana 125001, India

[2] Department of Pharmaceutical Sciences, G.J. University of Science and Technology, Hisar, Haryana 125001, India

Published online: 20 March 2018

Introduction

The need for pharmaceutical drugs is the core driving force for the extraordinary growth in metal-based drug development studies. The optimistic results revealed by tin complexes such as metallotherapeutics have inspired more precise research in this area [1–3]. Organotin(IV) complexes show uniqueness at synthetic and structural stages, and their application can be modified as a result of ligands attached to the central tin metal [4, 5]. Moreover, organotin(IV) complexes demonstrate the most assorted fragment of applications ranging from industrial, catalysis and therapetics due to their wide range of fascinating structural potential [6–11]. Some unique features of organotin(IV) complexes, such as thermodynamic and kinetic characteristics, coordination number variations, geometries, and intrinsic properties of the metal ion, have motivated research interest into finding use fore the varied approaches in diverse fields including agricultural, industrialized, and biomedical fields such as in wood preservatives, surface disinfectants, insecticides, antifouling agents [12–14]. Schiff bases show promising chemotherapeutic applications such as insecticidal, antibacterial, antifungal, anti-inflammatory and antitumor [15–17]. Nowadays, organotin(IV) complexes of Schiff bases are attractive scaffolds for novel drug discovery as a result of their remarkable biological activities. Schiff bases illustrate an expansive spectrum of applications owing to their ability to cleave microorganism DNA [18]. They are enormously studied due to structural varieties, flexibility, high thermal stability, and medical efficacy [19, 20]. Benzothiazoles are versatile fused heterocyclic scaffolds with extensive pharmaceutical applications. They are mainly found in bio-inorganic and medicinal chemistry with wide applications in drug discovery. A large number of therapeutic agents are synthesized with the help of a benzothiazole nucleus. In addition, benzothiazoles act as the core nucleus in various drugs due to their various activities and have attracted a great deal of interest due to their wide range of biological activity such as anticancer, antitubercular, anti-HIV, cardiovascular, local anaesthetic, anti-inflammatory, anticonvulsant and anti-diabetic. The therapeutic properties of the benzothiazoles have encouraged medicinal chemists to synthesize a large number of novel chemotherapeutic agents [21, 22]. Recently, substituted 2-arylbenzothiazoles have emerged as an imperative pharmacophore with a number of remedial and analytical properties due to their synthetic accessibility [23].

In pursuit of this, the present study focused on the synthesis, spectroscopic analysis, antimicrobial evaluation and QSAR studies of Schiff bases of 2-amino-6-substituted-benzothiazole derivatives and their respective organotin(IV) complexes.

Experimental

Materials and physical measurements

All chemicals were purchased from Sigma Aldrich and were used without further purification. All solvents were of analytical grade, received from Sigma Aldrich and

used after drying with standard procedures. IR spectra were recorded using a Shimadzu IR Affinity-I 8000 FT-IR spectrometer in the range 4000–400 cm^{-1}. NMR spectra of the compounds were recorded on 400 MHz using Bruker Avance II 400 MHz NMR spectrometer. ^{1}H, ^{13}C NMR and ^{119}Sn NMR were recorded using tetramethylsilane and tetramethyltin, respectively, as internal standard in DMSO-d_6. Tin was gravimetrically estimated as SnO_2 after decomposition with concentrated HNO_3 [24]. The melting points were recorded on an electrical heating coil apparatus and were uncorrected. The elemental analysis of the compounds was done using a Perkin Elmer 2400 instrument.

The compounds were assessed for in vitro antimicrobial activity against bacterial and fungal strains using serial dilution to evaluate MIC (minimum inhibitory concentration) [25]. Sabouraud dextrose broth and nutrient broth were used as growth media for fungal and bacterial strains, respectively, and test tubes with 1 mL of nutrient medium were autoclaved for 30 min at 121 °C. The stock solutions of compounds with a concentration of 100 μg/mL were prepared in DMSO and further diluted to concentrations of 50, 25, 12.5, 6.25, 3.12 and 1.56 μg/mL. One hundred microliters of freshly cultured strain in normal saline was transferred to each test tube for inoculation and incubated at 25 °C for 7 days for fungal strains and 37 °C for 24 h for bacterial strains. Each sample was assayed in triplicate, and the concordant MIC values were reported.

Pre-optimization of the structures of compounds **1–20** was done by the Molecular Mechanics Force Field (MM) process of Hyperchem 6.03 [26], and the resulting geometries were further developed by means of the semiempirical method Parametric Method-3 (PM-3). Geometric optimization was done by a gradient norm limit of 0.01 kcal/A°. The minimum energy structure of each molecule was used for the calculating physicochemical parameters using TSAR 3.3 software for Windows [27]. Regression analysis was done using the SPSS software package [28].

Synthesis of Schiff base ligands (1–4)

The methanolic solution of salicylaldehyde (5 mmol), 2-amino-6-substituted benzothiazoles (5 mmol), 2–3 drops of glacial acetic acid were refluxed together (30 mL) for about 5–6 h at room temperature. The solid obtained was dried, purified, washed with methanol and recrystallised with the mixture of methanol and chloroform (1:1, v/v). The purity of the compound was checked regularly with thin layer chromatography (TLC).

[1] (2-((6-ethoxybenzo[d]thiazol-2-ylimino)methyl)phenol) Yield: 82%; yellow solid; melting point: 180–182 °C; (Mol. Wt. 298.08); Anal. Calcd for $C_{16}H_{14}N_2O_2S$ (%): C, 64.41; H, 4.73; N, 9.39; O, 10.72; S, 10.75. Found: C, 64.03; H, 4.52; N, 9.04; O, 10.56; S, 10.49; IR (KBr pellets, cm^{-1}): 3430 (s, ν_{O-H}), 1618 (s, $\nu_{C=N}$), other bands (1204 s, 1036w, 969 s). ^{1}H NMR (DMSO-d_6, δ_H, ppm, 400 MHz): 11.72 (1H, s, O–H), 9.33 (1H, s, HC=N), 7.85 (1H, d, Ar–H, J = 8 Hz), 7.80 (1H, d, Ar–H, J = 8 Hz), 7.48 (1H, d, Ar–H), 7.07 (1H, d, Ar–H, J = 8 Hz), 7.02 (1H, t, Ar–H, J = 8 Hz), 7.00 (1H, t, Ar–H, J = 8 Hz), 6.95 (1H, s, Ar–H, J = 8 Hz), 4.14–4.08 (2H, q, OCH_2), 1.43–1.39 (3H, t, CH_3). ^{13}C NMR (DMSO-d6, δ_C, ppm,

100 MHz): 184.30, 171.00, 161.05, 145.34 (**C**=N), 135.52 126.65, 124.77, 123.97, 123.38, 122.94, 120.57, 115.65, 113.44, 112.56, 111.09 (s, Ar–C), 62.12 (s, C–OCH_2), 12.87 (s, C–CH_3).

[2] (2-((6-nitrobenzo[d]thiazol-2-ylimino)methyl)phenol) Yield: 84%; yellow solid; melting point: 168–170 °C; (Mol. Wt. 299.04); Anal. Calcd for $C_{14}H_9N_3O_3S$ (%): C, 56.18; H, 3.03; N, 14.04; O, 16.04; S, 10.71. Found: C, 55.96; H, 2.94; N, 13.96; O, 15.87; S, 10.35; IR (KBr pellets, cm^{-1}): 3338 (s, ν_{O-H}), 1617 (s, $\nu_{C=N}$), other bands (1209 s, 1035w, 975 s). ^{1}H NMR (DMSO-d_6, δ_H, ppm, 400 MHz): 11.64 (1H, s, O–H), 9.24 (1H, s, HC=N), 7.76 (1H, d, Ar–H, *J* = 8 Hz), 7.71 (1H, d, Ar–H, *J* = 8 Hz), 7.41 (1H, d, Ar–H, *J* = 8 Hz), 7.37 (1H, d, Ar–H, *J* = 8 Hz), 6.98 (1H, t, Ar–H, *J* = 8H), 6.91 (1H, t, Ar–H, *J* = 8 Hz), 6.88 (1H, s, Ar–H). ^{13}C NMR (DMSO-d_6, δ_C, ppm, 100 MHz): 182.12, 172.51, 158.87, 143.16 (**C**=N), 133.34, 124.47, 122.98, 122.59, 121.79, 121.20, 120.76, 118.39, 113.47, 111.29, 110.38 (s, Ar–C).

[3] (2-((6-methoxybenzo[d]thiazol-2-ylimino)methyl)phenol) Yield: 81%; yellow solid; melting point: 112–114 °C; (Mol. Wt. 284.06); Anal. Calcd for $C_{15}H_{12}N_2O_2S$ (%): C, 63.36; H, 4.25; N, 9.85; O, 11.25; S, 11.28. Found: C, 63.03; H, 3.96; N, 9.63; O, 10.97; S, 11.09. IR (KBr pellets, cm^{-1}): 3397 (s, ν_{O-H}), 1618 (s, $\nu_{C=N}$), other bands (1222 s, 1035w, 951 s). ^{1}H NMR (DMSO-d_6, δ_H, ppm, 400 MHz): 11.69 (1H, s, O–H), 9.29 (1H, s, HC=N), 7.81 (1H, d, Ar–H, *J* = 8 Hz), 7.76 (1H, d, Ar–H, *J* = 8 Hz), 7.47–7.41 (1H, m, Ar–H), 7.04 (1H, d, Ar–H, *J* = 8 Hz), 7.00 (1H, t, Ar–H, *J* = 8 Hz), 6.94 (1H, t, Ar–H, *J* = 8 Hz), 6.91 (1H, s, Ar–H), 4.08 (3H, s, OCH_3). ^{13}C NMR (DMSO-d6, δ_C, ppm, 100 MHz): 185.58, 162.63, 158.87, 146.92 (**C=N**), 137.10, 128.23, 126.74, 126.34, 125.55, 124.96, 124.52, 122.15, 117.23, 115.02, 114.14 (s, Ar–C), 61.82 (s, C–OCH_3).

[4] (2-((6-methylbenzo[d]thiazol-2-ylimino)methyl)phenol) Yield: 83%; yellow solid; melting point: 154–156 °C; (Mol. Wt. 268.07); Anal. Calcd for $C_{15}H_{12}N_2OS$ (%): C, 67.14; H, 4.51; N, 10.44; O, 5.96; S, 11.95. Found: C, 66.95; H, 4.38; N, 10.09; O, 5.65; S, 11.86. IR (KBr pellets, cm^{-1}): 3400 (s, ν_{O-H}), 1617 (s, $\nu_{C=N}$), other bands (1221 s, 1042w, 976 s). ^{1}H NMR (DMSO-d_6, δ_H, ppm, 400 MHz): 11.77 (1H, s, O–H), 9.37 (1H, s, HC=N), 7.90 (1H, d, Ar–H, *J* = 8 Hz), 7.85 (1H, d, Ar–H, *J* = 8 Hz), 7.54 (1H, m, Ar–H), 7.50 (1H, m, Ar–H), 7.12 (1H, t, Ar–H, *J* = 4 Hz), 7.04 (1H, t, Ar–H, *J* = 4 Hz), 7.01 (1H, s, Ar–H), 1.46 (3H, s, CH_3). ^{13}C NMR (DMSO-d6, δ_C, ppm, 100 MHz): 186.17, 162.93, 147.21, 137.40 (**C=N**), 128.53, 127.04, 126.64, 125.84, 125.26, 124.81, 122.45, 117.52, 115.31, 114.44 (s, Ar–C), 18.17 (s, CH_3).

Synthesis of complexes (5–20)

Diorganotin(IV) complexes were synthesized by reaction of corresponding Schiff base ligands (*R* = –OC_2H_5, –NO_2, –OCH_3, –CH_3) and the corresponding dialkl/aryltindichlorides (*R*' = Ph, Bu, Et, Me). A weighed amount of sodium (5 mmol) was added to the methanolic solution of prepared Schiff base ligands (5 mmol), and the reaction mixture was refluxed for 2 h to afford the sodium salts of the

corresponding Schiff bases. Dialkyl/aryltindichloride (5 mmol) was added to this sodium salt, and the reaction mixture was again refluxed for 9–10 h. Finally, after the solid salt separated out, it was filtered, washed with methanol and then collected. The excess solvent was evaporated over a rotary evaporator under reduced pressure to separate out the solid which was collected and washed with dry n-hexane. The collected solid was recrystallized with mixture of chloroform and diethylether (1:1, v/v).

[5] N-(2-(chlorodiphenylstannyloxy)benzylidene)-6-ethoxybenzo[d]thiazol-2-amine Yield: 79%; Yellow solid; melting point: 209–211 °C; (Mol. Wt. 606.02); Anal. Calc. for $C_{28}H_{23}ClN_2O_2SSn$ (%): C, 55.52; H, 3.83; Cl, 5.85; N, 4.62; O, 4.88; Sn, 19.60. Found: C, 55.34; H, 3.75; Cl, 5.56; N, 4.47; O, 4.89; Sn, 19.43. IR (KBr pellets, cm^{-1}): 1589 (s, $\nu_{C=N}$), 636 (m, ν_{Sn-N}), 520 (m, ν_{Sn-C}), 425 (w, ν_{Sn-O}), other bands (1222 s, 1027w, 982 s). ^{1}H NMR: (DMSO-d6, δ_H, ppm, 400 MHz): 9.68 (1H, s, HC=N), 8.09 (1H, s), 8.03 (1H, d, *J* = 8 Hz), 7.99 (1H, d, *J* = 8 Hz), 7.40–7.44 (10H, m), 7.39 (1H, d, *J* = 8 Hz), 7.35 (1H, d, *J* = 8 Hz), 7.32 (1H, d, *J* = 8 Hz), 7.22 (1H, d, *J* = 8 Hz), 4.12 (2H, q, OCH_2), 1.24 (3H, t, CH_3). ^{13}C NMR (DMSO-d6, δ_C, ppm, 100 MHz): 184.97, 172.88, 161.72, 150.98 (**C=N**), 145.96, 136.19, 133.65, 130.54, 127.42, 127.00, 125.84, 125.55, 124.64, 124.05, 123.61, 121.45, 117.39, 116.10, 112.05 (s, Ar–C), 66.56 (s, C–OCH_2), 13.55 (s, C–CH_3). ^{119} Sn NMR (DMSO-d6, δ_{Sn}, ppm, 149 MHz): − 326.35.

[6] N-(2-(dibutylchlorostannyloxy)benzylidene)-6-ethoxybenzo[d]thiazol-2-amine Yield: 76%; yellow solid; melting point: 201–203 °C; (Mol. Wt. 566.08); Anal. Calc. for $C_{24}H_{31}ClN_2O_2SSn$ (%): C, 50.95; H, 5.52; Cl, 6.27; N, 4.95; Sn, 20.98. Found: C, 50.65; H, 5.45; Cl, 6.01; N, 4.78; Sn, 20.72. IR (KBr pellets, cm^{-1}): 1601 (s, $\nu_{C=N}$), 621 (m, ν_{Sn-N}), 559 (m, ν_{Sn-C}), 436 (w, ν_{Sn-O}),other bands (1222 s, 1029w, 998 s). ^{1}H NMR: (DMSO-d6, δ_H, ppm, 400 MHz): 9.66 (1H, s, HC=N), 8.11 (1H, s), 8.03 (1H, d, *J* = 8 Hz), 7.86 (1H, d, *J* = 8 Hz), 7.82 (1H, d, *J* = 8 Hz), 7.65 (1H, d, *J* = 8 Hz), 7.45 (1H, d, *J* = 8 Hz), 7.35 (1H, d, *J* = 8 Hz), 4.12 (2H, q, OCH_2), 3.99 (4H, m, Bu), 3.56 (4H, m, Bu), 1.42 (3H, s, CH_3), 1.34 (4H, m), 0.89 (6H, t, Bu). ^{13}C NMR (DMSO-d6, δ_C, ppm, 100 MHz): 180.84, 168.75, 157.85, 146.85 (**C=N**), 141.82, 129.51, 126.40, 123.28, 121.41, 119.48, 119.48, 117.31, 113.26, 111.97, 107.92 (s, Ar–C), 62.43 (s, C–OCH_2), 33.50 (s, Bu–C), 23.20 (s, Bu–C), 19.42 (s, C–CH_3), 15.37 (s, Bu–C), 9.41 (s, Bu–C). ^{119}Sn NMR (DMSO-d6, δ_{Sn}, ppm, 149 MHz): − 267.14.

[7] N-(2-(chlorodimethylstannyloxy)benzylidene)-6-ethoxybenzo[d]thiazol-2-amine Yield: 77%; yellow brown; melting point: 214–216 °C; (Mol. Wt. 481.99); Anal. Calc. for $C_{18}H_{19}ClN_2O_2SSn$ (%): C, 44.89; H, 3.98; Cl, 7.36; N, 5.82; Sn, 24.65. Found: C, 44.76; H, 3.73; Cl, 7.09; N, 5.65; Sn, 24.21. IR (KBr pellets, cm^{-1}): 1591 (s, $\nu_{C=N}$), 608 (ν_{Sn-N}), 528 (ν_{Sn-C}), 457 (ν_{Sn-O}), other bands (1227 s, 1023w, 939 s). ^{1}H NMR: (DMSO-d6, δ_H, ppm, 400 MHz): 9.83, (1H, s, HC=N), 8.19 (1H, s), 8.11 (1H, d, *J* = 8 Hz), 7.93 (1H, d, *J* = 8 Hz), 7.89 (1H, d, *J* = 8 Hz), 7.70 (1H, d, *J* = 8 Hz), 7.50 (1H, d, *J* = 8 Hz), 7.30 (1H, d, *J* = 8 Hz, 4.05 (2H, q, OCH_2), 1.42 (3H, t, CH_3), 0.86 (6H, s, Me). ^{13}C NMR (DMSO-d6, δ_C, ppm, 100 MHz): 187.16, 175.07, 163.91, 153.17 (C=N), 148.14, 140.58, 138.83, 132.72, 129.60, 127.74, 125.80, 123.34,

119.58, 114.24, 108.88, 106.71,, (s, Ar–C), 63.71 (s, C–OCH_2), 29.52 (s, Me-C), 10.11 (s, C–CH_3). ^{119}Sn NMR (DMSO-d6, δ_{Sn}, ppm, 149 MHz): − 142.09.

[8] N-(2-(chlorodiethylstannyloxy)benzylidene)-6-ethoxybenzo[d]thiazol-2-amine Yield: 78%; yellow; melting point: 198–200 °C; (Mol. Wt. 510.02); Anal. Calc. for $C_{20}H_{23}ClN_2O_2SSn$ (%): C, 47.13; H, 4.55; Cl, 6.96; N, 4.95; Sn, 23.29. Found: C, 46.98; H, 4.24; Cl, 6.73; N, 5.32; Sn, 23.02. IR (KBr pellets, cm^{-1}): 1597 (s, $\nu_{C=N}$), 603 (m, ν_{Sn-N}), 534 (m, ν_{Sn-C}), 457 (w, ν_{Sn-O}), other bands (1216 s, 1024w, 924 s). ^{1}H NMR: (DMSO-d6, δ_H, ppm, 400 MHz): 8.89 (1H, s, HC=N), 8.11 (1H, s), 8.07 (1H, d, *J* = 8 Hz), 7.86 (1H, d, *J* = 8 Hz), 7.82 (1H, d, *J* = 8 Hz), 7.64 (1H, d, *J* = 8 Hz), 7.44 (1H, d, *J* = 8 Hz), 7.22 (1H, d, *J* = 8 Hz), 4.11 (2H, q, OCH_2), 1.42 (4H, t, CH_3), 1.08 (4H, t, Et), 0.90 (6H, m, Et). ^{13}C NMR (DMSO-d6, δ_C, ppm, 100 MHz): 184.59, 172.51, 161.35, 150.61 (**C=N**), 145.58, 133.27, 130.16, 127.04, 125.17, 123.24, 121.07, 117.02, 115.72, 111.68 (s, Ar–C), 63.31 (s, C–OCH_2), 26.96 (s, C–CH_3), 21.00 (s, Et-C), 15.91 (s, Et-C). ^{119}Sn NMR (DMSO-d6, δ_{Sn}, ppm, 149 MHz): − 172.95.

[9] N-(2-(chlorodiphenylstannyloxy)benzylidene)-6-nitrobenzo[d]thiazol-2-amine Yield: 78%, yellow solid; melting point: 189–191 °C; (Mol. Wt. 606.98); Anal. Calc. for $C_{26}H_{18}ClN_3O_3SSn$ (%): C, 51.47; H, 2.99; Cl, 5.84; N, 6.93; Sn, 19.57. Found: C, 51.21; H, 2.76; Cl, 5.49; N, 6.93; Sn, 19.31. IR (KBr pellets, cm^{-1}): 1580 (s, $\nu_{C=N}$), 606 (m, ν_{Sn-N}), 528 (m, ν_{Sn-C}), 455 (w, ν_{Sn-O}),other bands (1216 s, 1023w, 914 s) ^{1}H NMR (DMSO-d6, δ_H, ppm, 400 MHz): 9.81 (1H, s, HC=N), 8.54 (1H, s), 8.15 (1H, d, *J* = 8 Hz), 8.09–8.00 (10H, m), 7.98 (1H, d, *J* = 8 Hz), 7.84 (1H, t, *J* = 8 Hz), 7.61 (1H, d, *J* = 8 Hz), 7.58 (1H, d, *J* = 8 Hz), 7.27 (1H, d, *J* = 8 Hz) 7.22 (1H, d, *J* = 8 Hz). ^{13}C NMR (DMSO-d6, δ_C, ppm, 100 MHz): 184.00, 171.91, 160.75, 150.01 (**C=N**), 135.22, 132.67, 129.56, 126.44, 126.03, 124.86, 124.57, 123.08, 122.64, 120.47, 116.42, 115.13, 111.08 (s, Ar–C). ^{119}Sn NMR (DMSO-d6, δ_{Sn}, ppm, 149 MHz): − 322.35.

[10] N-(2-(dibutylchlorostannyloxy)benzylidene)-6-nitrobenzo[d]thiazol-2-amine Yield: 76%; yellow solid; melting point: 198–200 °C; (Mol. Wt. 567.04); Anal. Calc. for $C_{22}H_{26}ClN_3O_3SSn$ (%): C, 46.63; H, 4.62; Cl, 6.26; N, 7.42; Sn, 20.95. Found: C, 46.45; H, 4.34; Cl, 6.01; N, 7.26; Sn, 20.71. IR (KBr pellets, cm^{-1}): 1586 (s, $\nu_{C=N}$), 618 (m, ν_{Sn-N}), 593 (m, ν_{Sn-C}), 453 (w, ν_{Sn-O}), other bands (1216 s, 1026w, 917 s). ^{1}H NMR: (DMSO-d6, δ_H, ppm, 400 MHz): 10.06 (1H, s, HC=N), 8.07 (1H, s), 7.89 (1H, d, *J* = 8 Hz), 7.85 (1H, d, *J* = 8 Hz), 7.69 (1H, d, *J* = 8 Hz), 7.66 (1H, d, *J* = 8 Hz), 7.48 (1H, s, *J* = 8 Hz), 7.36 (1H, t, *J* = 8 Hz), 1.46 (4H, m), 1.38 (4H, m), 1.27 (4H, m), 0.91 (6H, t). ^{13}C NMR (DMSO-d6, δ_C, ppm, 100 MHz): 182.72, 170.63, 159.48, 148.73 (**C=N**), 143.71, 131.40, 128.29, 125.17, 123.30, 121.36, 119.20, 115.14, 113.80, 109.81(s, Ar–C), 33.89, 24.79, 19.13, 14.72 (s, Bu–C). ^{119}Sn NMR (DMSO-d6, δ_{Sn}, ppm, 149 MHz): − 280.75.

[11] N-(2-(chlorodimethylstannyloxy)benzylidene)-6-nitrobenzo[d]thiazol-2-amine Yield: 77%; brown solid; melting point: 192–194 °C; (Mol. Wt. 482.95); Anal. Calc. for $C_{16}H_{14}ClN_3O_3SSn$ (%): C, 39.83; H, 2.92; Cl, 7.35; N, 8.71; Sn, 24.60.

Found: C, 39.57; H, 2.78; Cl, 7.13; N, 8.71; Sn, 24.34. IR (KBr pellets, cm^{-1}): 1597 (s, $\nu_{C=N}$), 603 (ν_{Sn-N}), 534 (ν_{Sn-C}), 457 (ν_{Sn-O}), other bands (1216 s, 1024w, 924 s). ^{1}H NMR: (DMSO-d6, δ_H, ppm, 400 MHz): 9.70 (1H, s, HC=N), 8.22 (1H, s), 8.15 (1H, d, *J* = 8 Hz), 7.97 (1H, d, *J* = 8 Hz), 7.93 (1H, d, *J* = 8 Hz), 7.76 (1H, d, *J* = 8 Hz), 7.54 (1H, d, *J* = 8 Hz), 7.33 (1H, d, *J* = 8 Hz), 0.89 (6H, s, Me). ^{13}C NMR (DMSO-d6, δ_C, ppm, 100 MHz): 182.72, 170.63, 159.45, 148.73 (**C=N**), 143.71, 131.40, 128.29, 125.17, 123.30, 121.36, 119.20, 115.14, 113.85, 109.81 (s, Ar–C), 11.30 (s, Me-C). ^{119}Sn NMR (DMSO-d6, δ_{Sn}, ppm, 149 MHz): − 125.24.

[12] N-(2-(chlorodiethylstannyloxy)benzylidene)-6-nitrobenzo[d]thiazol-2-amine Yield: 79%; yellow solid; melting point: 187–189 °C; (Mol. Wt. 510.98); Anal. Calc. for $C_{18}H_{18}ClN_3O_3SSn$ (%): C, 42.34; H, 3.55; Cl, 6.94; N, 8.23; Sn, 23.25. Found: C, 42.06; H, 3.26; Cl, 6.76; N, 8.01; Sn, 23.01. IR (KBr pellets, cm^{-1}): 1580 (s, $\nu_{C=N}$), 606 (ν_{Sn-N}), 528 (ν_{Sn-C}), 455 (ν_{Sn-O}), other bands (1216 s, 1023w, 914 s). ^{1}H NMR: (DMSO-d6, δ_H, ppm, 400 MHz): 10.10 (1H, s, HC=N), 8.10 (1H, s), 8.11 (1H, d, *J* = 8 Hz), 7.93 (1H, d, *J* = 8 Hz), 7.89 (1H, d, *J* = 8 Hz), 7.71 (1H, d, *J* = 8 Hz), 7.50 (1H, d, *J* = 8 Hz), 7.30 (1H, d, *J* = 8 Hz), 1.16 (4H, q, Et), 0.97 (6H, t, Et). ^{13}C NMR (DMSO-d6, δ_C, ppm, 100 MHz): 183.70, 171.16, 160.45, 149.71 (**C=N**), 144.69, 132.38, 129.27, 126.15, 124.28, 122.34, 120.17, 116.12, 114.83, 110.78 (s, Ar–C), 24.69, 14.72 (s, Et-C). ^{119}Sn NMR (DMSO-d6, δ_{Sn}, ppm, 149 MHz): − 179.85.

[13] N-(2-(chlorodiphenylstannyloxy)benzylidene)-6-methoxybenzo[d]thiazol-2-amine Yield: 78%; yellow solid; melting point: 182–183 °C; (Mol. Wt. 592.00); Anal. Calc. for $C_{27}H_{21}ClN_2O_2SSn$(%): C, 54.81; H, 3.58; Cl, 5.99; N, 4.73; Sn, 20.06. Found: C, 54.72; H, 3.32; Cl, 5.78; N, 4.53; Sn, 19.89. IR (KBr pellets, cm^{-1}): 1600 (s, $\nu_{C=N}$), 604 (m, ν_{Sn-N}), 517 (m, ν_{Sn-C}), 412 (w, ν_{Sn-O}) other bands (1203 s, 1014w, 975 s). ^{1}H NMR: (DMSO-d6, δ_H, ppm, 400 MHz): 9.81 (1H, s, C=N), 8.09 (1H, s), 7.99 (1H, d, *J* = 8 Hz), 7.97–7.85 (10H, m), 7.61 (1H, d, *J* = 8 Hz), 7.59 (1H, d, *J* = 8 Hz), 7.27 (1H, d, *J* = 12 Hz), 7.22 (1H, t, *J* = 12 Hz), 7.11 (1H, d, *J* = 8 Hz), 4.04 (3H, s, OCH_3). ^{13}C NMR (DMSO-d6, δ_C, ppm, 100 MHz): 186.17, 174.08, 162.93, 152.18 (**C=N**), 147.16, 137.40, 134.85, 131.74, 128.62, 128.20, 127.04, 126.75, 125.84, 125.26, 124.81, 122.65, 118.59, 117.30, 113.26 (s, Ar–C), 62.11 (s, C–OCH_3). ^{119}Sn NMR (DMSO-d6, δ_{Sn}, ppm, 149 MHz): − 304.11.

[14] N-(2-(dibutylchlorostannyloxy)benzylidene)-6-methoxybenzo[d]thiazol-2-amine Yield: 76%, yellow solid; melting point: 197–199 °C; (Mol. Wt. 552.07); Anal. Calc. for $C_{23}H_{29}ClN_2O_2SSn$ (%): C, 50.07; H, 5.30; Cl, 6.43; N, 5.08; Sn, 21.52. Found: C, 49.94; H, 5.03; Cl, 6.23; N, 5.08; Sn, 21.41. IR (KBr pellets, cm^{-1}): 1604 (s, $\nu_{C=N}$), 607 (m, ν_{Sn-N}), 513 (m, ν_{Sn-C}), 419 (w, ν_{Sn-O}). other bands (1207 s, 1018w, 976 s). ^{1}H NMR: (DMSO-d6, δ_H, ppm, 400 MHz): 10.43 (1H, s, HC=N), 8.19 (1H, s), 8.05 (1H, d, *J* = 8 Hz), 7.87 (1H, d, *J* = 8 Hz), 7.83 (1H, d, *J* = 8 Hz), 7.64 (1H, t, *J* = 1 2 Hz), 7.46 (1H, t, *J* = 12 Hz), 7.36 (1H, d, *J* = 8 Hz), 4.12 (3H, s, OCH_3), 3.61 (4H, m), 3.55 (4H, m), 1.42 (4H, m), 1.35 (6H, t). ^{13}C NMR (DMSO-d6, δ_C, ppm, 100 MHz): 182.61, 170.31, 159.15, 148.41 (**C=N**), 143.38, 131.08, 127.96, 124.85, 122.98, 121.04, 118.87, 114.82, 113.53, 109.43 (s, Ar–C),

61.80 (s, OCH_3), 33.57, 24.47, 18.80, 14.39 (s, Bu–C). ^{119}Sn NMR (DMSO-d6, δ_{Sn}, ppm, 149 MHz): − 249.49.

[15] N-(2-(chlorodimethylstannyloxy)benzylidene)-6-methoxybenzo[d]thiazol-2-amine Yield: 75%; yellow solid; melting point: 178–180 °C; (Mol. Wt. 467.97); Anal. Calc. for $C_{17}H_{17}ClN_2O_2SSn$ (%): C, 43.67; H, 3.66; Cl, 7.58; N, 5.99; Sn, 25.39. Found: C, 43.42; H, 3.32; Cl, 7.21; N, 5.71; Sn, 25.12. IR (KBr pellets, cm^{-1}): 1596 (s, $\nu_{C=N}$), 612 (m, ν_{Sn-N}), 517 (m, ν_{Sn-C}), 415 (w, ν_{Sn-O}) other bands (1202 s, 1015w, 972 s). ^{1}H NMR: (DMSO-d6, δ_H, ppm, 400 MHz): 9.54 (1H, s, HC=N), 8.11 (1H, s), 7.86 (1H, d, *J* = 8 Hz), 7.82 (1H, d, *J* = 8 Hz), 7.65 (1H, d, *J* = 8 Hz), 7.43 (1H, t, *J* = 12 Hz), 7.22 (1H, t, *J* = 12 Hz), 7.09 (1H, d, *J* = 8 Hz), 4.11 (3H, s, OCH_3), 1.38 (6H, s, Me). ^{13}C NMR (DMSO-d6, δ_C, ppm, 100 MHz): 185.99, 173.50, 162.34, 151.60 (**C=N**), 146.57, 139.01, 136.81, 134.26, 131.15, 128.03, 126.17, 124.23, 122.06, 121.77, 118.01, 112.67, 107.31, 105.14 (s, Ar–C), 61.53 (s, C–OCH_3), 8.54 (s, Me-C). ^{119}Sn NMR (DMSO-d6, δ_{Sn}, ppm, 149 MHz): − 140.11.

[16] N-(2-(chlorodiethylstannyloxy)benzylidene)-6-methoxybenzo[d]thiazol-2-amine Yield: 78%; yellow solid; melting point: 195–197 °C; (Mol. Wt. 496.00); Anal. Calc. for $C_{19}H_{21}ClN_2O_2SSn$ (%): C, 46.04; H, 4.27; Cl, 67.15; N, 5.65; Sn, 23.95. Found: C, 45.89; H, 4.04; Cl, 7.02; N, 5.31; Sn, 23.72. IR (KBr pellets, cm^{-1}): 1602 (s, $\nu_{C=N}$), 605 (m, ν_{Sn-N}), 520 (m, ν_{Sn-C}), 409 (w, ν_{Sn-O}) other bands (1207 s, 1018w, 976 s). ^{1}H NMR: (DMSO-d6, δ_H, ppm, 400 MHz): 9.59 (1H, s, HC=N), 8.21 (1H, s), 8.02 (1H, d, *J* = 8 Hz), 7.89 (1H, d, *J* = 8 Hz), 7.84 (1H, d, *J* = 8 Hz), 7.69 (1H, t, *J* = 12 Hz), 7.39 (1H, t, *J* = 12 Hz), 7.25 (1H, d, *J* = 8 Hz), 4.11 (3H, s, OCH_3), 1.29 (4H, q), 0.92 (6H, t). ^{13}C NMR (DMSO-d6, δ_C, ppm, 100 MHz): 183.70, 171.61, 160.45, 149.71 (**C=N**), 144.69, 132.38, 129.27, 126.15, 124.28, 122.34, 120.17, 116.12, 114.83, 110.78 (s, Ar–C), 62.42 (s, C–OCH_3) 26.06, 15.02 (s, Et-C). ^{119}Sn NMR (DMSO-d6, δ_{Sn}, ppm, 149 MHz): − 176.09.

[17] N-(2-(chlorodiphenylstannyloxy)benzylidene)-6-methylbenzo[d]thiazol-2-amine Yield: 77%; yellow solid; melting point: 177–179 °C; (Mol. Wt. 576.01); Anal. Calc. for $C_{27}H_{21}ClN_2OSSn$ (%): C, 56.33; H, 3.68; Cl, 6.16; N, 4.87; Sn, 20.62. Found: C, 56.12; H, 3.42; Cl, 5.97; N, 4.56; Sn, 20.34. IR (KBr pellets, cm^{-1}): 1594 (s, $\nu_{C=N}$), 610 (m, ν_{Sn-N}), 504 (m, ν_{Sn-C}), 425 (w, ν_{Sn-O}),other bands (1211 s, 1019w, 974 s) ^{1}H NMR: (DMSO-d6, δ_H, ppm, 400 MHz): 9.42 (1H, s, HC=N), 8.12 (1H, s), 8.01 (1H, d, *J* = 8 Hz), 7.93–7.87 (10H, m), 7.65 (1H, d, *J* = 8 Hz), 7.61 (1H, d, *J* = 8 Hz), 7.29 (1H, d, *J* = 12 Hz), 7.21 (1H, t, *J* = 12 Hz), 7.14 (1H, d, *J* = 8 Hz), 1.35 (3H, s, CH_3) ppm. ^{13}C NMR (DMSO-d6, δ_C, ppm, 100 MHz) 185.88, 173.79, 162.63, 151.89 (**C=N**), 146.86, 137.10, 134.56, 131.44, 128.32, 127.91, 126.74, 125.55, 124.96, 124.52, 122.35, 118.30, 117.01, 112.96 (s, Ar–H), 11.89 (s, C–CH_3). ^{119}Sn NMR (DMSO-d6, δ_{Sn}, ppm, 149 MHz): − 300.75.

[18] N-(2-(dibutylchlorostannyloxy)benzylidene)-6-methylbenzo[d]thiazol-2-amine Yield: 78%; yellow solid; melting point: 165–167 °C; (Mol. Wt. 536.07); Anal. Calc. for $C_{23}H_{29}ClN_2OSSn$ (%): C, 51.57; H, 5.46; Cl, 6.62; N, 5.46; Sn, 22.16. Found: C, 51.32; H, 5.35; Cl, 6.45; N, 5.04; Sn, 21.98. IR (KBr pellets, cm^{-1}): 1603

(s, $\nu_{C=N}$), 610 (m, ν_{Sn-N}), 519 (m, ν_{Sn-C}), 410 (w, ν_{Sn-O}), other bands (1213 s, 1021w, 973 s). ^{1}H NMR: (DMSO-d6, δ_H, ppm, 400 MHz): 9.75 (1H, s, HC=N), 8.21 (1H, s), 8.07 (1H, d, *J* = 8 Hz), 7.86 (1H, d, *J* = 8 Hz), 7.81 (1H, d, *J* = 8 Hz), 7.68 (1H, t, *J* = 1 2 Hz), 7.48 (1H, t, *J* = 12 Hz), 7.38 (1H, d, *J* = 8 Hz), 4.05 (4H, m, Bu), 3.64 (4H, m, Bu), 1.49 (4H, m, Bu), 1.41 (6H, t, Bu), 1.28 (3H, s, CH_3). ^{13}C NMR (DMSO-d6, δ_C, ppm, 100 MHz): 181.81, 169.72, 158.57, 147.82 (**C=N**), 142.80, 130.49, 127.38, 124.26, 122.39, 120.45, 118.29, 114.23, 112.94, 108.90 (s, Ar–C), 32.98, 23.88, 18.22, 13.81, 9.73 (s, C–CH_3). ^{119}Sn NMR (DMSO-d6, δ_{Sn}, ppm, 149 MHz): − 252.95.

[19] N-(2-(chlorodimethylstannyloxy)benzylidene)-6-methylbenzo[d]thiazol-2-amine Yield: 79%, yellow solid; melting point: 172–174 °C; (Mol. Wt. 451.98); Anal. Calc. for $C_{17}H_{17}ClN_2OSSn$ (%): C, 45.22; H, 3.79; Cl, 7.85; N, 6.20; Sn, 26.29. Found: C, 44.10; H, 3.61; Cl, 7.68; N, 6.01; Sn, 25.96. IR (KBr pellets, cm^{-1}): 1602 (s, $\nu_{C=N}$), 608 (m, ν_{Sn-N}), 508 (m, ν_{Sn-C}), 413 (w, ν_{Sn-O}), other bands (1220 s, 1025w, 976 s). ^{1}H NMR (DMSO-d6, δ_H, ppm, 400 MHz): 9.75 (1H, s, HC=N), 8.14 (1H, s), 7.87 (1H, d, *J* = 8 Hz), 7.83 (1H, d, *J* = 8 Hz), 7.67 (1H, d, *J* = 8 Hz), 7.45 (1H, t, *J* = 12 Hz), 7.25 (1H, t, *J* = 12 Hz), 7.11 (1H, d, *J* = 8 Hz), 1.37 (3H, s, CH_3), 0.86 (6H, s, Me). ^{13}C NMR (DMSO-d6, δ_C ppm, 100 MHz): 182.40, 172.31, 159.15, 148.41 (**C=N**), 143.38, 131.08, 127.96, 124.85, 122.98, 121.04, 118.87, 114.82, 113.53, 109.48 (s, Ar–H), 18.80 (s, C–CH_3), 10.97 (s, Me-C). ^{119}Sn NMR (DMSO-d6, δ_{Sn}, ppm, 149 MHz): − 126.09.

[20] N-(2-(chlorodiethylstannyloxy)benzylidene)-6-methylbenzo[d]thiazol-2-amine Yield: **7**6%, yellow solid; melting point: 186–188 °C; (Mol. Wt. 480.01); Anal. Calc. for $C_{19}H_{21}ClN_2OSSn$ (%): C, 47.58; H, 4.41; Cl, 6.69; N, 5.58; Sn, 24.75. Found: C, 47.32; H, 4.23; Cl, 6.34; N, 5.34; Sn, 24.54. IR (KBr pellets, cm^{-1}): 1610 (s, $\nu_{C=N}$), 619 (m, ν_{Sn-N}), 504 (m, ν_{Sn-C}), 409 (w, ν_{Sn-O}), other bands (1218 s, 1024w, 975 s). ^{1}H NMR (DMSO-d6, δ_H, ppm, 400 MHz): 9.89 (1H, s, HC=N), 8.25 (1H, s), 8.05 (1H, d, *J* = 8 Hz), 7.92 (1H, d, *J* = 8 Hz), 7.87 (1H, d, *J* = 8 Hz), 7.71 (1H, t, *J* = 12 Hz), 7.42 (1H, t, *J* = 12 Hz), 7.27 (1H, d, *J* = 8 Hz), 1.43 (3H, s, CH_3), 1.12 (4H, q, Et), 0.91 (6H, t, Et). ^{13}C NMR (DMSO-d6, δ_C ppm, 100 MHz): 183.09, 171.00, 159.84, 149.10 (C=N), 144.07, 131.77, 128.65, 125.67, 123.67, 121.73, 119.56, 115.51, 114.22, 110.17 (Ar–C), 25.15 (s, C–CH_3), 15.08, 8.81 (s, Et-C). ^{119}Sn NMR (DMSO-d6, δ_{Sn} ppm, 149 MHz): − 175.24.

Results and discussion

Synthetic aspects

The reaction of salicylaldehyde with 2-amino-6-substituted-benzothiazole (where *R* = $-OC_2H_5$, $-NO_2$, $-OCH_3$, $-CH_3$) leads to the formation of (1-[(6-substituted-benzothiazol-2-ylimino)-methyl]-naphthalen-2-ol) (**1–4**). The sodium salt of the Schiff base ligands was prepared using Na metal, which was then reacted with R_2SnCl_2, yielding complexes **5–20**. These were isolated as coloured compounds that

are soluble in DMSO and less soluble in chloroform. The purity of the compounds was checked by TLC. The synthetic protocol of the Schiff base ligands and their diorganotin(IV) complexes is shown in Scheme 1.

IR spectra

FT-IR spectra of all the ligands and the complexes were recorded using KBr pellets. The coordination sites of the ligands were assigned by comparing IR spectra of the corresponding Schiff bases with their corresponding diorganotin(IV) complexes. The presence of a hydroxyl group in the Schiff base ligands was confirmed by the appearance of a broad absorption band at 3316–3287 cm^{-1} due to ν (OH). The absorption band of medium intensity with stretching frequency at 1623–1612 cm^{-1} was attributed to the ν (C=N) of azomethine group in the ligands. The broad absorption band of the hydroxyl group disappeared due to the deprotonation of phenolic group in the complexes suggesting bonding of oxygen atom to the central tin atom. The absorption band for the azomethine group was shifted by 10–24 cm^{-1} towards lower frequencies with medium intensity in complexes suggesting coordination of nitrogen atom to the tin atom. The other bands appeared at their usual positions. The absorption bands were observed in the ranges 619–602, 521–504, 425–403 cm^{-1} attributed to ν (Sn–C), ν (Sn–O), ν (Sn–N) vibrations respectively, and suggesting coordination of carbon, oxygen and nitrogen to the central tin atom [29, 30].

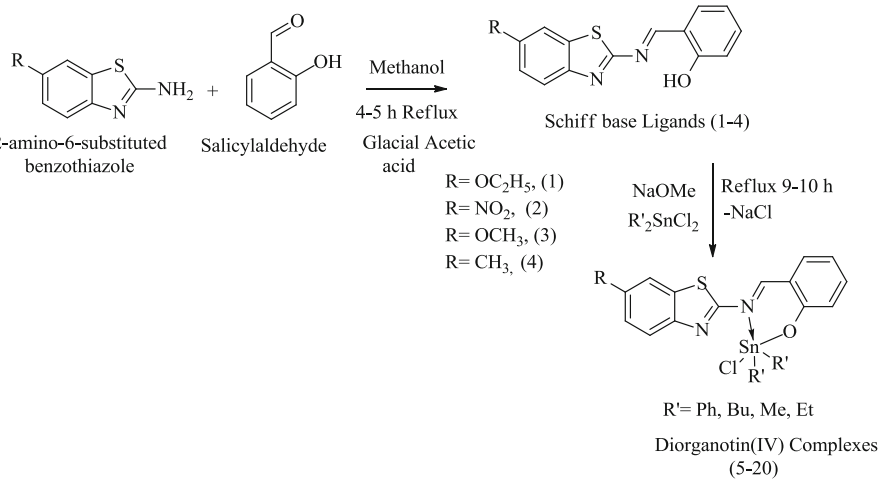

Scheme 1 Scheme for the synthesis of Schiff base ligands and organotin(IV) complexes

NMR spectroscopy

^{1}H NMR

The ^{1}H, ^{13}C, ^{119}Sn NMR spectra of the ligands and the complexes were recorded in DMSO. The ^{1}H NMR spectra of the compounds are based on integration values, coupling constants and chemical shifts. The signal in the range δ 11.77–11.64 ppm was assigned to phenolic proton in Schiff base ligands. A signal in the range δ 9.37–9.24 ppm revealed the presence of azomethine protons in the ligands, confirming the condensation of benzothiazole derivatives with salicylaldehyde. The signals at δ 7.89–6.88 ppm were assigned to the aryl protons of the ligands and the signals due to aliphatic protons appeared in the range δ 4.14–1.39 ppm due to the presence of strong electron withdrawing groups in the compounds. The ^{1}H NMR spectra of the complexes were compared with that of the ligands on the basis of coupling constants, integration and chemical shift values. All the diorganotin(IV) complexes showed the absence of signal due to phenolic proton suggesting the deprotonation of the phenolic proton and coordination to the tin atom. The proton signals of azomethine group were slightly shifted which may be due to the coordination of nitrogen atom of imino moeity to the tin atom leading to a significant deshielding effect. The signals of aryl and alkyl groups were observed in the expected regions as reported earlier [31–33].

^{13}C NMR

In the ^{13}C NMR spectra of the ligands, the signal due to carbon attached to the phenolic group was observed at δ 186.17–182.12 ppm. The carbons attached to thiazole group appeared at δ 162.93–143.16 ppm due to presence of nitrogen and sulfur. The carbon attached to the azomethine group was appeared in the range δ 137.40–133.34 ppm. The carbons attached to the aromatic ring were appeared in the expected region in the range δ 128.53–110.38 ppm in ligands. The chemical shift values of carbon attached to aliphatic group appeared in the region from δ 62.12–12.87 ppm in ligands. In the ^{13}C NMR spectra of the complexes, the signal due to phenolic groups was shifted due to bonding of oxygen to the central tin atom indicating formation of complexes. The carbons attached to thiazole group were shifted because of deshielding effect due to presence of nearby azomethine nitrogen. The azomethine carbon was shifted downfield on complexation indicating involvement of nitrogen atom in coordination to the central tin atom. The aromatic and aliphatic carbons were appeared at their usual positions [34–36].

^{119}Sn NMR

A sharp singlet appeared in the ^{119}Sn spectra of the compounds in the range δ − 326.35 to − 300.75 ppm for phenyl, δ − 280.75 to − 249.49 ppm for butyl, δ − 179.85 to − 170.76 ppm for ethyl, and δ − 142.09 to − 125.24 ppm for methyl complexes. These chemical shifts revealed the formation of pentacoordinated tin

centres in the complexes. The phenyltin complexes showed high field chemical shift values due to anisotropic shielding effects, as well as the pi interactions [34–37].

In vitro antimicrobial activity

The in vitro antimicrobial activity of all synthesized compounds was evaluated against Gram negative bacteria, *E. coli*, *P. aeruginosa,* Gram positive bacteria, *B. cereus*, *S. aureus*, and fungi, *A. niger, A. flavus*. Ciprofloxacin and fluconazole were used as standard drugs for antibacterial and antifungal activity, respectively. The serial dilution method was used for the evaluation of antimicrobial activity. The results of antimicrobial activity in terms of MIC (minimum inhibitory concentration in μM/mL) are presented in Table 1. The results of antibacterial and antifungal activity revealed that the compound **5** was found to be the most active against all microbial strains. The ligands were found to be least active. The order of antimicrobial activity was found Ph > Bu > Et > Me. From the observed results, it

Table 1 In vitro antimicrobial activity of Schiff bases derived from 2-amino-6-substituted benzothiazoles with salicylaldehyde and their diorganotin(IV) complexes

Compound	MIC (μM/mL)					
	E.coli	*P.aeruginosa*	*B.cereus*	*S. aureus*	*A. niger*	*A. flavus*
1	0.0419	0.0209	0.0419	0.0209	0.0104	0.0209
2	0.0209	0.0209	0.0418	0.0209	0.0104	0.0209
3	0.0220	0.0220	0.0440	0.0220	0.0110	0.0220
4	0.0233	0.0233	0.0465	0.0233	0.0116	0.0233
5	0.0101	0.0048	0.0048	0.0024	0.0024	0.0048
6	0.0110	0.0055	0.0055	0.0057	0.0027	0.0055
7	0.0245	0.0061	0.0122	0.0123	0.0061	0.0061
8	0.0130	0.0065	0.0130	0.0130	0.0065	0.0065
9	0.0103	0.0051	0.0051	0.0026	0.0026	0.0051
10	0.0220	0.0055	0.0055	0.0027	0.0027	0.0055
11	0.0122	0.0061	0.0122	0.0063	0.0061	0.0061
12	0.0129	0.0064	0.0129	0.0067	0.0064	0.0064
13	0.0211	0.0052	0.0052	0.0026	0.0026	0.0053
14	0.0113	0.0056	0.0056	0.0059	0.0113	0.0056
15	0.0126	0.0126	0.0126	0.0126	0.0031	0.0063
16	0.0267	0.0134	0.0134	0.0134	0.0034	0.0067
17	0.0108	0.0054	0.0054	0.0027	0.0027	0.0054
18	0.0116	0.0058	0.0058	0.0060	0.0029	0.0058
19	0.0253	0.0063	0.01263	0.0126	0.0063	0.0063
20	0.0276	0.0069	0.0138	0.0138	0.0069	0.0069
Ciprofloxacin	0.0047	0.0047	0.0047	0.0047	–	–
Fluconazole	–	–	–	–	0.0102	0.0102

was observed that there was a remarkable boost in the activity of complexes than the ligands. The increase in the antimicrobial activity of synthesized complexes may be due to chelation, as it tends to formulate ligands to operate as more influential and better antimicrobial agents [38–40].

QSAR analysis

QSAR analysis for the in vitro antimicrobial activity and structural descriptors coding for various molecular properties of the diorganotin(IV) complexes of Schiff bases derived from 2-amino-6-substituted-benzothiazoles described by Hansch and Fujita [41] using the linear free energy relationship model (LFER). The pMIC (–log MIC), i.e. the negative logarithm of observed antimicrobial activity (MIC, Table 2) was taken for QSAR study. The structural descriptors were calculated for diorganotin(IV) complexes of Schiff bases derived from 2-amino-6-substituted benzothiazoles and salicylaldehyde are presented in Table 3 [42–48].

In the present study, a dataset of synthesized compounds was subjected to linear regression analysis to correlate antimicrobial activity with structural quantifiers, i.e. molecular descriptors. The inter-relationship between structural quantifiers and

Table 2 In vitro antimicrobial activity (pMIC) values of Schiff bases derived from 2-amino-6-substituted benzothiazoles with salicylaldehyde and their diorganotin(IV) complexes

Compounds	pMICec	PMICpa	pMICbc	pMICsa	pMICan	pMICaf
1	1.378	1.679	1.378	1.679	1.981	1.679
2	1.680	1.680	1.379	1.680	1.982	1.680
3	1.658	1.658	1.357	1.658	1.960	1.658
4	1.633	1.633	1.332	1.633	1.935	1.633
5	1.986	2.288	2.288	2.589	2.589	2.288
6	1.957	2.258	2.258	2.241	2.559	2.258
7	1.610	2.213	1.911	1.911	2.213	2.213
8	1.887	2.189	1.887	1.887	2.189	2.189
9	1.987	2.289	2.289	2.590	2.590	2.289
10	1.656	2.259	2.259	2.560	2.560	2.259
11	1.912	2.214	1.912	2.196	2.214	2.214
12	1.888	2.189	1.888	2.172	2.189	2.189
13	1.675	2.278	2.278	2.579	2.579	2.278
14	1.946	2.248	2.248	2.230	1.946	2.248
15	1.899	1.899	1.899	1.899	2.502	2.201
16	1.573	1.874	1.874	1.874	2.477	2.176
17	1.964	2.266	2.266	2.567	2.567	2.266
18	1.933	2.235	2.235	2.217	2.536	2.235
19	1.597	2.200	1.898	1.898	2.200	2.200
20	1.558	2.161	1.859	1.859	2.161	2.161
Std.	2.610	2.610	2.610	2.610	2.640	2.640

Table 3 Molecular descriptors for Schiff bases derived from 2-amino-6-substituted benzothiazoles with salicylaldehyde and their diorganotin(IV) complexes

Compounds	$^{0}\chi$	$^{0}\chi^{v}$	$^{1}\chi$	$^{1}\chi^{v}$	$^{2}\chi$	$^{2}\chi^{v}$	$^{3}\chi$	$^{3}\chi^{v}$	$\square_1$	$\square_2$	$\square_3$	*R*	*J*	*W*	Te	*M*
1	14.66	12.37	10.26	7.50	8.92	5.47	1.14	0.60	15.88	7.51	4.05	10.26	1.29	1045.00	− 3488.69	2.67
2	14.82	11.52	10.13	6.89	9.27	5.31	1.44	0.64	15.88	7.05	3.85	10.13	1.31	1027.00	− 3687.89	7.12
3	13.95	11.66	9.76	6.91	8.54	5.24	1.14	0.60	14.92	6.84	3.62	9.76	1.30	897.00	− 3332.90	2.69
4	13.24	11.25	9.22	6.80	8.37	5.38	1.23	0.69	13.96	6.19	3.37	9.22	1.30	769.00	− 3012.93	1.38
5	24.09	23.69	17.15	20.13	15.09	20.15	2.06	4.73	26.60	12.70	6.53	17.15	1.10	3977.00	− 5605.39	1.91
6	22.11	23.16	15.06	21.13	12.93	22.28	2.00	5.65	25.62	13.03	7.78	15.06	1.41	3045.00	− 5206.50	2.10
7	19.28	20.33	13.06	19.13	11.43	21.97	2.00	5.65	21.70	10.16	5.76	13.06	1.38	2069.00	− 4583.21	2.11
8	17.86	18.91	11.94	19.70	11.47	22.06	2.64	9.34	19.75	8.79	5.74	11.94	1.35	1681.00	− 4271.70	6.62
9	24.25	22.84	17.03	19.52	15.44	20.00	2.35	4.78	26.60	12.24	6.36	17.03	1.11	3945.00	− 5804.79	6.66
10	22.27	22.31	14.94	20.51	13.28	22.12	2.30	5.69	25.62	12.46	7.50	14.94	1.42	3017.00	− 5405.69	7.50
11	19.44	19.48	12.94	18.51	11.78	21.82	2.30	5.69	21.70	9.67	5.54	12.94	1.39	2045.00	− 4782.40	7.47
12	18.03	18.06	11.82	19.09	11.82	21.91	2.93	9.38	19.75	8.35	5.49	11.82	1.36	1659.00	− 4470.85	5.07
13	23.38	22.98	16.65	19.54	14.71	19.92	2.06	4.73	25.64	12.03	6.12	16.65	1.11	3616.00	− 5449.67	4.08
14	21.40	22.45	14.56	20.54	12.55	22.05	2.00	5.65	24.64	12.30	7.26	14.56	1.42	2746.00	− 5050.72	1.99
15	18.57	19.62	12.56	18.54	11.05	21.75	2.00	5.65	20.73	9.47	5.30	12.56	1.39	1836.00	− 4427.43	2.06
16	17.16	18.21	11.44	19.11	11.09	21.83	2.64	9.34	18.78	8.13	5.25	11.44	1.36	1478.00	− 4115.92	6.41
17	22.68	22.57	16.12	19.43	14.54	20.06	2.14	4.83	24.68	11.37	5.88	16.12	1.12	3289.00	− 5129.69	4.23
18	20.69	22.04	14.03	20.43	12.38	22.19	2.09	5.75	23.66	11.57	7.00	14.03	1.42	2477.00	− 4730.74	2.41
19	17.86	19.21	12.03	18.43	10.88	21.88	2.09	5.75	19.75	8.79	5.04	12.03	1.39	1629.00	− 4107.45	2.40
20	16.45	17.80	10.90	19.00	10.92	21.97	2.72	9.44	17.81	7.49	4.99	10.90	1.36	1299.00	− 3795.94	5.54

antimicrobial activities was analyzed on the basis of regression analysis and correlation matrix constructed for antifungal activity of synthesized compounds against *A. flavus* is presented in Table 4. The correlation of different molecular descriptors with antimicrobial activities is presented in Table 5. An overview of the entire dataset demonstrated high colinearity ($r > 0.8$) between structural quantifiers. The high correlation was observed between first order molecular connectivity index, $^{1}\chi$ and Randic parameter, R ($r = 1.000$), zero order molecular connectivity index, $^{0}\chi$ and lectronic energy, Ele.E ($r = 0.997$), zero order molecular connectivity index, $^{0}\chi$ and nuclear repulsion energy, Nu.E ($r = 0.997$), and least inter-relationship was observed between valence zero order molecular connectivity index, $^{0}\chi^{v}$ and dipole moment, μ ($r = 0.008$), first order molecular connectivity index, $^{1}\chi$ and dipole moment, μ ($r = 0.008$) and Randic parameter, R and dipole moment, μ ($r = 0.008$). The correlation matrix highlighted the role of various molecular connectivity indices (Topological descriptors) in modulation of antibacterial and antifungal activity of the synthesized complexes.

The QSAR model for antifungal potential of synthesized compounds against *A. flavus* depicted that structural descriptors, valence first order molecular connectivity index ($^{1}\chi^{v}$) is responsible for the control of antifungal activity (Eq. 1)

QSAR model for antifungal activity against A. flavus

$$\mathrm{pMIC_{af}} = 0.045\,^{1}\chi^{v} + 1.350 \quad (1)$$

$n = 20$ $r = 0.990$ $r^2 = 0.980$ $q^2 = 0.977$ $s = 0.034$ $F = 881.67$

Topological indices are numerical quantifiers of molecular topology and are sensitive to bonding pattern, symmetry, heteroatom content, as well as degree of complexity of atomic neighborhoods. The first-order molecular connectivity topological index ($^{2}\chi$) represents the molecules with branched structure [49]. The QSAR model represented by Eq. 1 for antifungal activity against *A. flavus* has high r, r^2, q^2 and F values and a low s value, which indicates that the results of the predicted antifungal activity will be reliable. The validity of the QSAR model was examined by leave-one-out (LOO) method, which states that the mathematical models are valid if they have q^2 value greater than 0.5, and both of these models meet this criterion [50]. The statistical significance of the validity of Eq. 1 was also assessed by drawing two plots, one between observed and predicted antifungal activity (Fig. 1) and the other between the observed and residual antifungal activity (Fig. 2), and both of these plots support the validity of the QSAR model represented by Eq. 1.

QSAR model for antibacterial activity against B. cereus

$$\mathrm{pMIC_{bc}} = 0.080\,^{0}\chi^{v} + 0.405 \quad (2)$$

$n = 20$ $r = 0.989$ $r^2 = 0.977$ $q^2 = 0.973$ $s = 0.053$ $F = 774.243$

QSAR model for antibacterial activity against S. aureus

$$\mathrm{pMIC_{sa}} = 0.157\,^{2}\chi + 0.240 \quad (3)$$

$n = 20$ $r = 0.963$ $r^2 = 0.926$ $q^2 = 0.913$ $s = 0.096$ $F = 226.314$

Table 4 Correlation matrix of structural descriptors for Schiff bases derived from 2-amino-6-substituted benzothiazoles with salicylaldehyde and their diorganotin(IV) complexes for antibacterial activity against *S. aureus*

	$^{0}\chi$	$^{0}\chi^{v}$	$^{1}\chi$	$^{1}\chi^{v}$	$^{2}\chi$	$^{2}\chi^{v}$	$^{3}\chi$	$^{3}\chi^{v}$	κ_1	κ_2	R	Te	Ele.E	NuE	μ	pMICaf
$^{0}\chi$	1.000															
$^{0}\chi^{v}$	0.948	1.000														
$^{1}\chi$	0.991	0.910	1.000													
$^{1}\chi^{v}$	0.785	0.931	0.713	1.000												
$^{2}\chi$	0.976	0.915	0.974	0.777	1.000											
$^{2}\chi^{v}$	0.681	0.863	0.595	0.984	0.672	1.000										
$^{3}\chi$	0.429	0.587	0.339	0.808	0.517	0.844	1.000									
$^{3}\chi^{v}$	0.308	0.534	0.212	0.797	0.373	0.851	0.956	1.000								
κ_1	0.994	0.959	0.975	0.807	0.950	0.706	0.427	0.324	1.000							
κ_2	0.962	0.921	0.948	0.737	0.888	0.626	0.292	0.215	0.982	1.000						
R	0.991	0.910	1.000	0.713	0.974	0.595	0.339	0.212	0.975	0.948	1.000					
Te	− 0.989	− 0.928	− 0.971	− 0.780	− 0.963	− 0.681	− 0.461	− 0.325	− 0.986	− 0.949	− 0.971	1.000				
Ele.E	− 0.997	− 0.950	− 0.987	− 0.784	− 0.962	− 0.679	− 0.404	− 0.293	− 0.997	− 0.976	− 0.987	0.985	1.000			
NuE	0.997	0.951	0.987	0.783	0.960	0.678	0.399	0.290	0.997	0.977	0.987	− 0.982	− 1.000	1.000		
M	0.056	0.008	0.008	0.126	0.149	0.149	0.490	0.329	0.034	− 0.070	0.008	− 0.146	− 0.027	0.016	1.000	
pMICaf	0.836	0.952	0.773	0.990	0.832	0.968	0.780	0.740	0.847	0.768	0.773	− 0.831	− 0.831	0.830	0.138	1.000

Table 5 Correlation of molecular descriptors with antimicrobial activity of Schiff bases derived from 2-amino-6-substituted benzothiazoles with salicylaldehyde and their diorganotin(IV) complexes

	pMICec	pMICpa	pMICbc	pMICsa	pMICan	pMICaf
$^{0}\chi$	0.641	0.855	0.957	0.953	0.795	0.836
$^{0}\chi^{v}$	0.615	0.923	0.989	0.859	0.785	0.952
$^{1}\chi$	0.621	0.803	0.923	0.952	0.787	0.773
$^{1}\chi^{v}$	0.536	0.911	0.906	0.691	0.693	0.990
$^{2}\chi$	0.628	0.850	0.935	0.962	0.805	0.832
$^{2}\chi^{v}$	0.477	0.866	0.826	0.580	0.620	0.968
$^{3}\chi$	0.348	0.687	0.583	0.427	0.453	0.780
$^{3}\chi^{v}$	0.255	0.612	0.510	0.257	0.365	0.740
κ_1	0.643	0.863	0.966	0.932	0.780	0.847
κ_2	0.616	0.800	0.929	0.885	0.729	0.768
κ_3	0.590	0.841	0.925	0.779	0.667	0.833
R	0.621	0.803	0.923	0.952	0.787	0.773
J	− 0.159	− 0.085	− 0.174	− 0.450	− 0.326	− 0.019
W	0.615	0.777	0.903	0.953	0.775	0.736
Te	− 0.647	− 0.844	− 0.935	− 0.947	− 0.775	− 0.831
Ele.E	− 0.639	− 0.849	− 0.960	− 0.942	− 0.787	− 0.831
NuE	0.637	0.848	0.961	0.940	0.787	0.830
LUMO	− 0.425	− 0.467	− 0.417	− 0.615	− 0.384	− 0.420
HOMO	0.053	0.259	0.333	0.105	0.240	0.327
M	0.000	0.126	0.051	0.167	0.121	0.138

QSAR model for antibacterial activity against P. aeruginosa

$$\mathrm{pMIC_{pa}} = 0.054\,{}^{0}\chi^{v} + 1.064 \quad (4)$$

$n = 20$ $r = 0.923$ $r^2 = 0.852$ $q^2 = 0.833$ $s = 0.097$ $F = 103.509$

QSAR model for antifungal activity against A. niger

$$\mathrm{pMIC_{an}} = 0.097\,{}^{2}\chi + 1.148 \quad (5)$$

$n = 20$ $r = 0.805$ $r^2 = 0.648$ $q^2 = 0.601$ $s = 0.155$ $F = 33.198$

In the case of antibacterial activity of synthesized compounds against *B. cereus*, the QSAR model represented by Eq. 2 was obtained, which pointed out the involvement of valence zero order molecular connectivity index ($^{0}\chi^{v}$) in deciding the pattern of antibacterial activity against *B. cereus*. This model (Eq. 2) also has high r, r^2, q^2 and F values and low s values, which suggests the high prediction reliability of this model. The coefficient of valence zero order molecular index ($^{0}\chi^{v}$) is positive which indicated that antibacterial potential (Table 3) of synthesized compounds will increase with increase in values of $^{0}\chi^{v}$ (Table 4) and the same can be confirmed from the results that compounds 5 and 9 with high $^{0}\chi^{v}$ values (23.688 and 22.836, respectively) have high antibacterial activity (2.288 and 2.289 μM/mL,

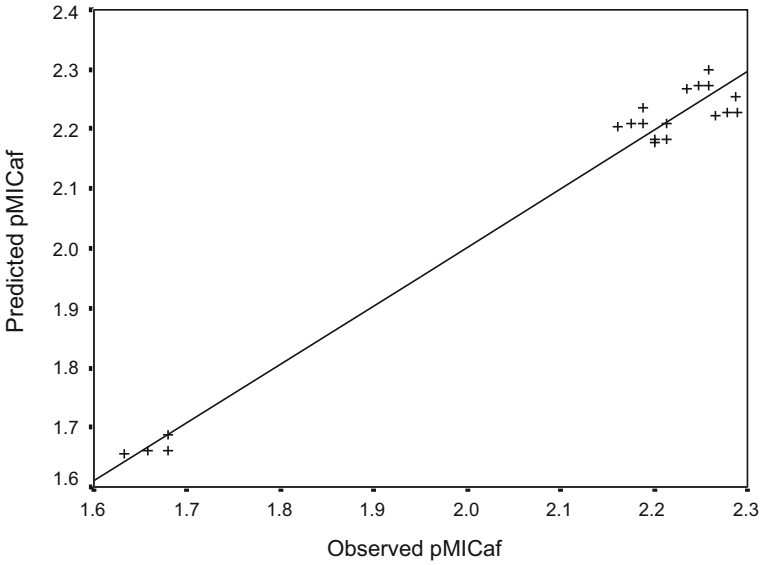

Fig. 1 Plot of observed $pMIC_{af}$ against the predicted $pMIC_{af}$ for the linear regression model developed by Eq. 1

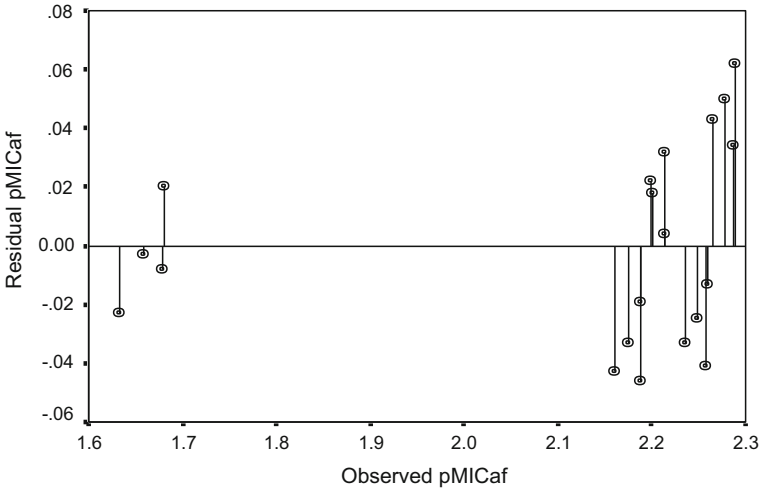

Fig. 2 Plot of residual $pMIC_{af}$ against the observed $pMIC_{af}$ for the linear regression model developed by Eq. 1

respectively), and compounds 3, 4 and 19 with low $^{0}\chi^{v}$ values (11.660, 11.251 and 17.799, respectively) have low antibacterial activity.

The QSAR model for antibacterial activity of synthesized compounds against *S. aureus* revealed the importance of second-order molecular connectivity index ($^{2}\chi$) in altering the antibacterial activity (Eq. 3). The coefficient of molecular descriptors

Table 6 Observed, predicted and residual antimicrobial activity of Schiff bases derived from 2-amino-6-substituted benzothiazoles with salicylaldehyde and their diorganotin(IV) complexes

Compounds	pMICaf			PMICbc			pMICsa			pMICpa			pMICan		
	Obs	Pre	Res	Obs	Pre	Res	Obs	Pre	Res	Obs	Pre	Res	Obs	Pre	Res
1	1.679	1.687	− 0.008	1.378	1.400	− 0.022	1.679	1.641	0.038	1.679	1.728	− 0.049	1.981	2.015	− 0.034
2	1.680	1.660	0.020	1.379	1.331	0.048	1.680	1.696	− 0.016	1.680	1.682	− 0.002	1.982	2.049	− 0.067
3	1.658	1.661	− 0.003	1.357	1.343	0.014	1.658	1.581	0.077	1.658	1.690	− 0.032	1.960	1.978	− 0.018
4	1.633	1.656	− 0.023	1.332	1.310	0.022	1.633	1.555	0.078	1.633	1.668	− 0.035	1.935	1.962	− 0.027
5	2.288	2.254	0.034	2.288	2.310	− 0.022	2.589	2.608	− 0.019	2.288	2.336	− 0.048	2.589	2.613	− 0.024
6	2.258	2.299	− 0.041	2.258	2.267	− 0.009	2.241	2.270	− 0.029	2.258	2.308	− 0.050	2.559	2.404	0.155
7	2.213	2.209	0.004	1.911	2.040	− 0.129	1.911	2.034	− 0.123	2.213	2.156	0.057	2.213	2.258	− 0.045
8	2.189	2.235	− 0.046	1.887	1.926	− 0.039	1.887	2.041	− 0.154	2.189	2.080	0.109	2.189	2.262	− 0.073
9	2.289	2.227	0.062	2.289	2.241	0.048	2.590	2.663	− 0.073	2.289	2.290	− 0.001	2.590	2.647	− 0.057
10	2.259	2.272	− 0.013	2.259	2.199	0.060	2.560	2.324	0.236	2.259	2.262	− 0.003	2.560	2.438	0.122
11	2.214	2.182	0.032	1.912	1.971	− 0.059	2.196	2.089	0.107	2.214	2.110	0.104	2.214	2.292	− 0.078
12	2.189	2.208	− 0.019	1.888	1.858	0.030	2.172	2.096	0.076	2.189	2.034	0.155	2.189	2.296	− 0.107
13	2.278	2.228	0.050	2.278	2.253	0.025	2.579	2.549	0.030	2.278	2.298	− 0.020	2.579	2.576	0.003
14	2.248	2.273	− 0.025	2.248	2.210	0.038	2.230	2.210	0.020	2.248	2.270	− 0.022	1.946	2.367	− 0.421
15	2.201	2.183	0.018	1.899	1.983	− 0.084	1.899	1.974	− 0.075	1.899	2.118	− 0.219	2.502	2.221	0.281
16	2.176	2.209	− 0.033	1.874	1.869	0.005	1.874	1.981	− 0.107	1.874	2.042	− 0.168	2.477	2.225	0.252
17	2.266	2.223	0.043	2.266	2.220	0.046	2.567	2.522	0.045	2.266	2.276	− 0.010	2.567	2.560	0.007
18	2.235	2.268	− 0.033	2.235	2.178	0.057	2.217	2.183	0.034	2.235	2.248	− 0.013	2.536	2.350	0.186
19	2.200	2.178	0.022	1.898	1.950	− 0.052	1.898	1.948	− 0.050	2.200	2.096	0.104	2.200	2.205	− 0.005
20	2.161	2.204	− 0.043	1.859	1.836	0.023	1.859	1.955	− 0.096	2.161	2.020	0.141	2.161	2.209	− 0.048

($^2\chi$) in Eq. 3 is positive, which indicates that antibacterial activity will increase with increasing values of $^2\chi$ and vice versa, and the same can be verified from the results presented in Tables 3 and 4.

In the case of antibacterial potential of synthesized compounds against *P. aeruginosa*, the computational model represented by Eq. 4 was obtained, and this model emphasized that valence zero-order molecular connectivity index ($^0\chi^v$) was the determinant factor for the antibacterial activity of the synthesized compounds. The antifungal activity of synthesized compounds against *A. niger* was governed by second-order molecular connectivity index ($^2\chi$) and positive coefficient of $^2\chi$ signifies that the antifungal activity against *A. niger* will increase with increase in $^2\chi$ values. No statistically valid model was obtained for antibacterial potential of synthesized compounds against *E. coli*. Similar to the QSAR model represented by Eqs. 1, 2–5 have high r, r^2, q^2 and F values and low s values, and the comparison of observed and predicted antimicrobial potential of synthesized compounds (Table 6) revealed that they have low residual values, thus confirming the statistical validity of these models [51–53].

Acknowledgements The authors are grateful to the CIL, Guru Jambheshwar University of Science and Technology, Hisar and SAIF, Punjab University, Chandigarh for providing IR and NMR facilities. One of the authors, Ms. Aarti Ahlawat, is thankful to UGC, New Delhi for providing financial assistance. The authors are thankful to Dr. Namita Singh, Department of Bio and Nanotechnology, Guru Jambheshwar University of Science and technology, Hisar for providing microbial strains.

Compliance with ethical standards

Conflict of interest The authors declare that they have no conflict of interest.

References

1. M.A. Salam, M.A. Hussein, I. Ramli, M.S. Islam, J. Organomet. Chem. **813**, 71 (2016)
2. L. Xu, M. Hong, Y. Yang, J. Cui, C. Li, J. Coord. Chem. **69**(17), 2598 (2016)
3. R.A. Haque, M.A. Salam, M.A. Arafath, J. Coord. Chem. **68**(16), 2953 (2015)
4. Y.Y. Zhang, R.F. Zhang, S.L. Zhang, S. Cheng, Q.L. Li, C.L. Ma, Dalton Trans. **45**(20), 8412 (2016)
5. M. Hong, H. Yin, X. Zhang, C. Li, C. Yue, S. Cheng, J. Organomet. Chem. **724**, 23 (2013)
6. G.M. Treich, S. Nasreen, A. Mannodi Kanakkithodi, R. Ma, M. Tefferi, J. Flynn, Y. Cao, R. Ramprasad, G.A. Sotzing, ACS Appl. Mater. Interfaces **8**(33), 21270 (2016)
7. M.C. García-López, B.M. Munoz-Flores, R. Chan-Navarro, V.M. Jiménez-Pérez, I. Moggio, E. Arias, A. Rodríguez-Ortega, M.E. Ochoa, J. Organomet. Chem. **806**, 68 (2016)
8. A. Tyagi, G. Kedarnath, A. Wadawale, V.K. Jain, M. Kumar, B. Vishwanadh, RSC Adv. **5**(77), 62882 (2015)
9. T.A. Grusenmeyer, A.W. King, J.T. Mague, J.J. Rack, R.H. Schmehl, Dalton Trans. **43**(47), 17754 (2014)
10. F.A. Shah, S. Sabir, K. Fatima, S. Ali, I. Qadri, C. Rizzoli, Dalton Trans. **44**(22), 10467 (2015)
11. M. Roy, S. Roy, K.S. Singh, J. Kalita, S.S. Singh, New J. Chem. **40**(2), 1471 (2016)
12. A.D. Garnovskii, I.S. Vasilchenko, D.A. Garnovskii, B.I. Kharisov, J. Coord. Chem. **62**(2), 151 (2009)
13. A. Chilwal, P. Malhotra, A.K. Narula, Phosphorus Sulfur Silicon Relat. Elem. **189**, 410 (2014)
14. H.L. Siddiqui, A. Iqbal, S. Ahmad, G.W. Weaver, Molecules **11**, 206 (2006)
15. M. Nath, P.K. Saini, A. Kumar, Appl. Organometal. Chem. **23**, 434 (2009)

16. T.S. Basu Baul, W. Rynjah, E. Rivarola, A. Lycka, M. Holcapek, R. Jirásko, D. de Vos, J.B.L.A. Ray, J. Organomet. Chem. **691**, 4850 (2006)
17. W. Rehman, M.K. Baloch, A. Badshah, Eur. J. Med. Chem. **43**, 2380 (2008)
18. H.L. Singh, J. Singh, Bioinorg. Chem. Appl. **2014**, 1 (2014)
19. J. Devi, S. Devi, A. Kumar, Heteroat. Chem. **27**(6), 361 (2016)
20. A.A.R. Despaigne, G.L. Parrilha, J.B. Izidoro, P.R. da Costa, R.G. Santos, O.G. Piro, E.E. Castellano, W.R. Rocha, H. Beraldo, Eur. J. Med. Chem. **50**, 163 (2012)
21. A. Kamal, M.A.H. Syed, S.M. Mohammed, Expert Opin. Ther. Pat. **25**(3), 335 (2015)
22. S. Seth, Anti-Inflamm. Anti-Allergy Agents Med. Chem. **14**(2), 98 (2015)
23. A.A. Weekes, A.D. Westwell, Curr. Med. Chem. **16**(19), 2430 (2009)
24. A.K. Sonika, O.P. Narula, H.K. Vermani, A.S. Sharma, J. Sarpal, Organometal. Chem. **470**(1–2), 67 (1994)
25. D.F. Spooner, G. Sykes, *Methods in Microbiology* (Academic Press, London, 1972)
26. Hyperchem 6.0, Hypercube Inc., Gainesville (1993)
27. TSAR 3D Version 3.3, Oxford Molecular Limited (2000)
28. SPSS for Windows, version 10.05, SPSS Inc Bangalore, India (1999)
29. M.K. Rauf, M.A. Saeed, M. Imtiaz-ud-Din, A. Bolte, B.Mirza Badshah, J. Organomet. Chem. **693**(18), 3043 (2008)
30. M.A. Abdellah, S.K. Hadjikakou, N. Hadjiliadis, M. Kubicki, T. Bakas, N. Kourkoumelis, Y.V. Simos, S. Karkabounas, M.M. Barsan, I.S. Butler, Bioinorg. Chem. Appl. **2009**, 1 (2009)
31. Sonika Nidhi, R. Malhotra, Phosphorus Sulfur Silicon Relat. Elem. **186**, 1449 (2011)
32. S. Asija, N. Malhotra, R. Malhotra, Phosphorus Sulfur Silicon Relat. Elem. **187**, 1510 (2012)
33. K. Singh, Y. Kumar, R.K. Pundir, Synth. React. Inorg. Met. Org. Chem. **40**, 836 (2010)
34. A. Ahlawat, V. Singh, S. Asija, Chem. Pap. **71**, 2195 (2017)
35. P. Khatkar, S. Asija, Phosphorus Sulfur Silicon Relat. Elem. **192**, 446 (2017)
36. P. Khatkar, S. Asija, N. Singh, J. Serb. Chem. Soc. **82**, 13 (2017)
37. R. Malhotra, A. Ravesh, V. Singh, Phosphorus Sulfur Silicon Relat. Elem. **192**, 73 (2017)
38. J. Devi, S. Devi, A. Kumar, Monatsh. Chem. **147**, 2195 (2016)
39. L.C. Dias, G.M. Lima, J.A. Takahashi, J.D. Ardisson, Appl. Organomet. Chem. **29**, 305 (2015)
40. L. Czympiel, J.M. Lekeu, C. Hegemann, S. Mathur, Inorg. Chim. Acta **455**, 197 (2017)
41. C. Hansch, T. Fujita, J. Am. Chem. Soc. **86**, 1616 (1964)
42. C. Hansch, A. Leo, S.H. Unger, K.H. Kim, D. Nikaitani, E.J. Lien, J. Med. Chem. **16**(11), 1207 (1973)
43. L.B. Kier, L.H. Hall, *Molecular Connectivity in Chemistry and Drug Research* (Academic Press, New York, 1976)
44. M. Randic, J. Am. Chem. Soc. **97**, 6609 (1975)
45. A.T. Balaban, Chem. Phys. Lett. **89**, 399 (1982)
46. H. Wiener, J. Am. Chem. Soc. **69**, 17 (1947)
47. M. Randic, Croat. Chem. Acta **66**, 289 (1993)
48. V. Lather, A.K. Madan, Bioorg. Med. Chem. **13**, 1599 (2005)
49. A. Golbraikh, A. Tropsha, J. Mol. Graph. Model. **20**, 269 (2002)
50. A. Kumar, B. Narasimhan, D. Kumar, Bioorg. Med. Chem. **15**, 4113 (2007)
51. V. Judge, B. Narasimhan, M. Ahuja, Med. Chem. Res. **21**(3), 1363 (2012)
52. L.B. Kier, L.H. Hall, in *Topological Indices and Related Descriptors in QSAR and QSPR*, ed. by J. Devillers, A.T. Balaban (Gordon and Breach Science Publishers, Amsterdam, 1999), p. 455
53. M. Karelson, V.S. Lobanov, A.R. Katritzky, Chem. Rev. **96**(3), 1027 (1996)